

DEVELOPMENT OF SEISMIC ISOLATION TABLE COMPOSED OF AN X-Y TABLE AND WIRE ROPE ISOLATORS

Hirokazu SHIMODA¹, Norio NAGA², Haruo SHIMOSAKA³ And Kenichiro OHMATA⁴

SUMMARY

In this study, a new type of isolation table composed of an X-Y table and wire rope isolators is developed. The wire rope isolator has both stiffness and Coulomb damping in x, y and z directions. The isolation table is simple in construction, and has about the same stiffness and damping in all directions on the horizontal plane. Resisting force characteristics of the X-Y table and the wire rope isolator and fatigue strength of the wire rope isolator are measured. The seismic response of a weight or a two-degree-of freedom furnishings model on the isolation table are also measured employing an electro-hydraulic type shaking table, and the experimental results are compared with the calculated results.

INTRODUCTION

Several types of isolation tables have been developed to isolate electronic equipment, precision instruments, artistic handicrafts, etc. from earthquake or external vibration [Takagami, 1986],[Kashiwazaki, 1989],[Iwata, 1990],[Fujita, 1992]. In order to develop the isolation table, which is simple in construction and low in cost, the authors have devised the isolation tables composed of circular arc beams and magnetic damping, and confirmed their effects of isolation theoretically and experimentally [Furuya, 1992],[Watanabe, 1996]. The isolation tables developed by the authors, however, are not suitable for an object which is heavy in weight and high in centre of gravity since it can not carry large overturning moment. In this study, a new type of seismic isolation table composed of an X-Y table and wire isolators is proposed. It is designed with a low height and a high load capacity to overcome the disadvantage mentioned above. The resisting force characteristics of the X-Y table and the isolators and fatigue strength of the isolator are examined experimentally. The seismic responses of an isolation object placed on the isolation table are also measured employing an electro-hydraulic type shaking table, and the experimental results are compared with the calculated results.

CONSTRUCTION OF ISOLATION TABLE

Construction of a wire isolator is shown in Fig. 1. The wire rope isolator is composed of stranded wire ropes, which is made from cold-drawn wires, and a pair of clamping plates for keeping a helical shape of the wire rope as shown in Fig. 1. It has both compliance and Coulomb damping in x, y and z directions since elastic deflection and sliding friction are simultaneously produced by rubbing between the wires when the wire rope is loaded. It is also characterized by an approximately linear spring and long stroke in compression and by a hardening spring in tension when it is loaded in z direction. Therefore, compliance of the wire rope isolator is utilized only in negative direction of z axis for the isolation table in this paper.

The isolation table developed by the authors is shown in Fig. 2. Table board (1) is supported by two sets of two linear ball bearings(6) for X direction which is carried by two sets of two linear ball bearings(6') for Y direction, so that the table board can perform a movement in all directions on the horizontal plane. Two sets of eight connected wire rope isolators in series for X direction (8) are installed between a pair of end plates (5) which are mounted on the under surface of the table board. The clamping plates of the wire rope isolator are in face-to-face contact each other, and both end faces of a series of the wire rope isolators are free form connections to the

¹ Department of Mechanical Engineering, Meiji University, Kawasaki, Japan

² Graduate Student, Meiji University, Kawasaki, Japan

³ Department of Mechanical Engineering, Meiji University, Kawasaki, Japan

⁴ Department of Mechanical System Science and Engineering, Meiji University, Kawasaki, Japan

end plate and the load plate (2) which is mounted to the linear ball bearings. Arrangement of the wire rope isolators is kept by a pair of guide bar (4) which put through each hole of the clamping plates. Therefore, the wire rope isolators can carry only the compressive load when an X directional movement is produced between the table board and the base board (3). Such a spring action is identical with the action of a compressive helical spring which is free at both ends. Similarly, two sets of eight wire rope isolators for Y direction (8') are installed in series between a pair of end plates (5') which are mounted on the upper surface of the base board (3). Therefore, the wire rope isolators can carry only the Y directional compressive load.

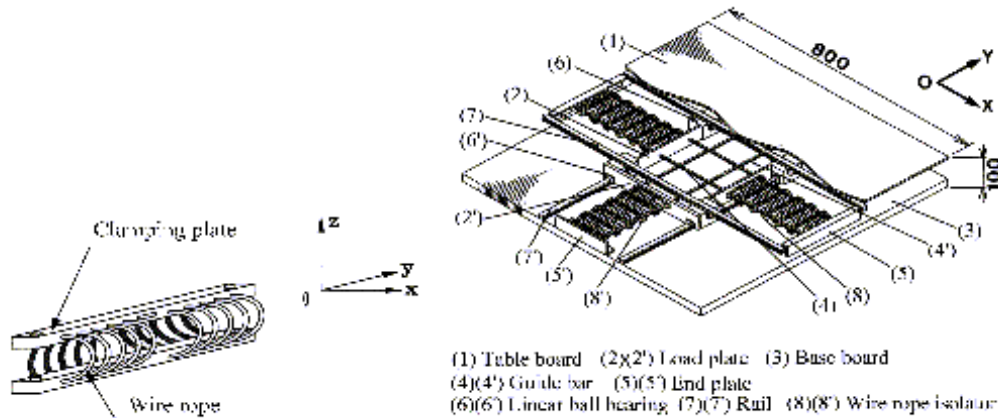


Fig. 1 Wire rope isolator

Fig. 2 Isolation table

CHARACTERISTICS OF ISOLATION TABLE

Resisting force characteristics of the X-Y table

In order to clarify the force-displacement characteristics of the X-Y table, the displacement and the resisting force between the base board installed on a vibrator and the table board attached to a rigid wall are examined. The displacement and the resisting force are measured by an inductance type displacement transducer, and a load cell respectively. Figure 3 shows the resisting force characteristics of the X-Y table under sinusoidal displacement of frequency 0.5, 1.0, 1.5 and 2.0 Hz. These results show that the X-Y table has the friction force $f_0 = 11\text{N}$ and damping force $c_0 = 48\text{Ns/m}$ in X direction and has $f_0 = 19\text{N}$ and $c_0 = 80\text{Ns/m}$ in Y direction. The friction force correspond to friction coefficient $\mu = 0.014$ and μ can be easily changed by oversize of balls in the linear ball bearing. The differences in f_0 and c_0 between in X and Y directions is mainly due to the difference in preload of the linear ball bearings.

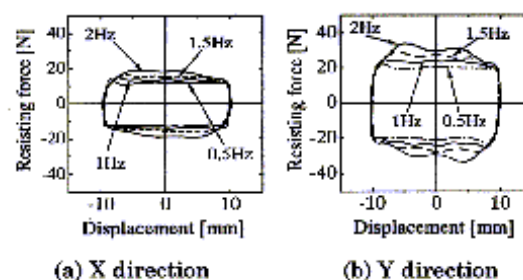


Fig. 3 Resisting force characteristics of the X-Y table

Stiffness and damping characteristics of the wire rope isolator

The static stiffness of a wire rope isolator in z direction measured by a material testing machine is shown in Fig. 4. Since the wire rope isolator has the feature that can be deformed like a hardening spring in tension, whereas like an approximately linear spring and has a sufficient stroke in compression, the isolation table in this paper is designed to utilize only its compressive compliance. Figure 5 shows the resisting force characteristics of a wire rope isolator, and four and eight connected wire rope isolators. It is seen from Fig.5 that the eight connected

wire rope isolators has stiffness $k_w=1280\text{N/m}$ and friction force $f_w=12.8\text{N}$. In order to clarify resisting force characteristics of the wire rope isolator, the relationship between displacement and force of the wire rope isolator under sinusoidal displacement of total amplitude 3 mm and frequency 1, 2, 3, 5 or 7 Hz in pulsating compression is measured. Hysteresis loops for the frequency 1 and 7 Hz, which are shown in Fig. 6, show that the wire rope isolator has no viscous damping.

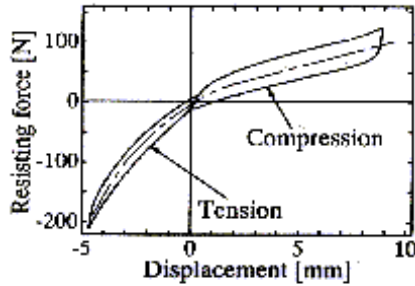


Fig. 4 Resisting force characteristics of the wire rope isolator in compression and tension

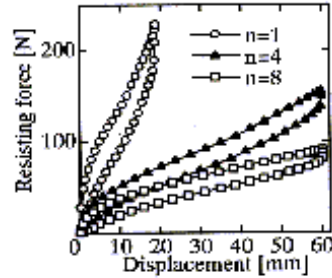


Fig. 5 Resisting force characteristics of the isolators

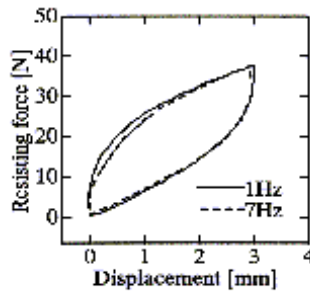


Fig. 6 Resisting force characteristics of the isolator

Fatigue strength of the wire rope isolator

In order to clarify the fatigue strength of the wire rope isolator, the change of resisting force under the sinusoidal displacement of total amplitude 15 mm or 19 mm and frequency 2 Hz in pulsating compression is examined. Total amplitude 15 mm and 19 mm correspond to 75% and 95% of the full stroke of the wire rope isolator respectively. The experimental results of fatigue strength, which is shown in Fig. 7, show that the resisting force of the wire rope isolator can be still maintained at a sufficient level for the number of load cycle up to 5×10^5 .

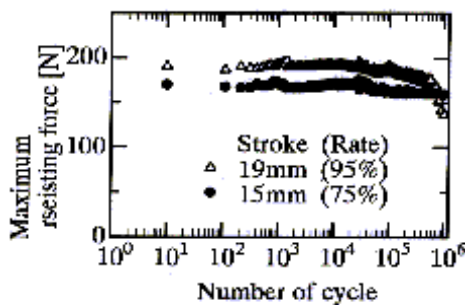


Fig. 7 Results of the fatigue life tests

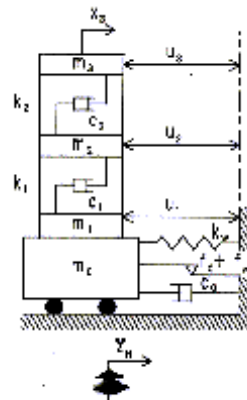


Fig. 8 Analytical model

SEISMIC RESPONSE ANALYSIS

Analytical model and equation of motion

Figure 8 shows the two-degree-of freedom-furnishing model having three concentrated masses on the isolation table. A tall furnishing like a locker, which is partitioned into three shelves, is chosen as an isolation object in the analytical model. Temporary stay of the X-Y table, which is produced by the kinetic friction force between the linear ball bearings and rails, must be taken into account in this analysis. If the furnishing model on the isolation table is subjected to a horizontal acceleration input \ddot{z}_H in X direction, the equations of motion the analytical model are given by the following expressions:

(1) Case of stay

$$\begin{aligned} u_1 &= \text{const}, \dot{u}_1 = 0, \ddot{u}_1 = 0 \\ m_2 \ddot{u}_2 + c_1 \dot{u}_2 + c_2 (\dot{u}_2 - \dot{u}_3) + k_1 (u_2 - u_1) + k_2 (u_2 - u_3) &= -m_2 \ddot{z}_H \\ m_3 \ddot{u}_3 + c_2 (\dot{u}_3 - \dot{u}_2) + k_2 (u_3 - u_2) &= -m_3 \ddot{z}_H \end{aligned} \quad (1)$$

(2) Case of movement

$$\begin{aligned} (m_0 + m_1) \ddot{u}_1 + c_0 \dot{u}_1 + c_1 (\dot{u}_1 - \dot{u}_2) + k_w u_1 + k_1 (u_1 - u_2) + (f_0 + f_w) \text{sign}(\dot{u}_1) &= -(m_0 + m_1) \ddot{z}_H \\ m_2 \ddot{u}_2 + c_1 (\dot{u}_2 - \dot{u}_1) + c_2 (\dot{u}_2 - \dot{u}_3) + k_1 (u_2 - u_1) + k_2 (u_2 - u_3) &= -m_2 \ddot{z}_H \\ m_3 \ddot{u}_3 + c_2 (\dot{u}_3 - \dot{u}_2) + k_2 (u_3 - u_2) &= -m_3 \ddot{z}_H \end{aligned} \quad (2)$$

(3) Switching condition from stay to movement

$$\left| (m_0 + m_1) \ddot{z}_H - c_1 \dot{u}_2 + k_w u_1 + k_1 (u_1 - u_2) \right| \geq f_0 + f_w \quad (3)$$

(4) Switching condition from movement to stay

$$\dot{u}_1 = 0, \text{ and } \left| (m_0 + m_1) (\dot{u}_1 + \ddot{z}_H) - c_1 \dot{u}_2 + k_w u_1 + k_1 (u_1 - u_2) \right| \leq f_0 + f_w \quad (4)$$

in which $\text{sign}(\dot{u}_1)$ is signum which is 1, 0 or -1 according to sign of \dot{u}_1

where m_1, m_2 and m_3 are the mass of the base, the 1st and the 2nd shelf of the furnishings respectively, c_1 and c_2 are the equivalent viscous damping coefficient, and k_1 and k_2 are the stiffness of the 1st and the 2nd shelf of the furnishings respectively. And, m_0, c_0 and f_0 are the mass, the equivalent viscous damping coefficient and the kinetic friction force of the X-Y table respectively, k_w and f_w are the stiffness and the kinetic friction force of the eight connected wire rope isolators respectively, and u_1, u_2 and u_3 are the relative displacement of m_1, m_2 and m_3 to the ground respectively. Above equations can be applied for horizontal acceleration input in Y direction. m_2, m_3, k_2, k_3, c_2 and c_3 in equations (1) and (2) can be neglected where the isolation object is regarded as a concentrated mass m_1 .

Response spectrum

Equations (1), (2), (3) and (4) are programmed employing a continuous system simulation language (FUJITSU SLCS5), and El Centro (1940) N-S and AKITA (1983) N-S normalized to be 2.0 m/s^2 at the maximum acceleration are used as input seismic waves. The calculated results of the maximum response acceleration for the concentrated mass 20 to 810 kg including the mass of the table board are shown in Fig. (9) and (10). These figures also contain the calculated results for several values of μ in order to examine the effect of μ on the response spectrum. It is apparent from Figs. (9) and (10) that the acceleration ratios are fall in the range of 0.3 to 0.9 for the various mass.

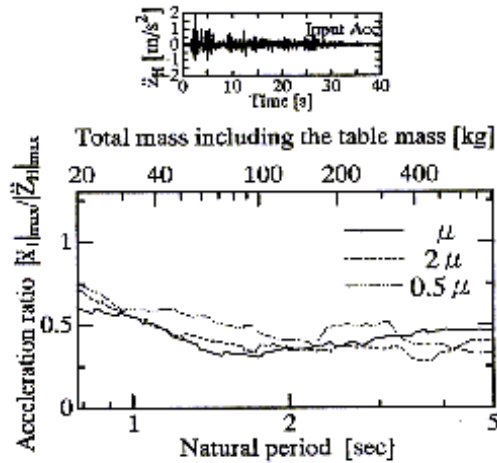


Fig. 9 Response spectrum (El Centro NS)

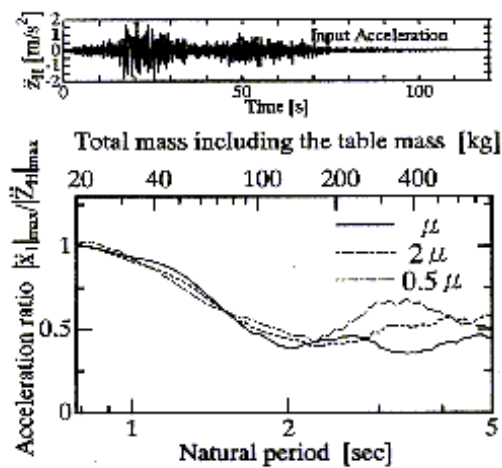


Fig. 10 Response spectrum (Akita NS)

SHAKING TABLE TEST

Case of concentrated mass

Figure 11 shows the concentrated mass of 100 kg on the isolation table installed on an electro-hydraulic type shaking table. The acceleration of the table board \ddot{x}_1 and the relative displacement u_1 are measured by an accelerometer and a 3-D motion real-time analysis system (LAVIC, MTEC Co.) respectively. Seismic waves are inputted in the direction $\theta=0$ (X direction), 30, 45, 60 or 90° (Y direction).

Table 1 shows the experimental and calculated maxima of the responses for the input seismic waves of El Centro (1940) N-S and AKITA (1983) N-S normalized to be 0.5, 1.0 and 2.0 m/s^2 at the maximum acceleration. Figure 12 shows the experimental and calculated response waves for the above input normalized to be 1.0 m/s^2 at the maximum acceleration. Table 1 and Fig. 12 lead to the following: (1) The effect of the isolation table becomes larger as the input acceleration increases. (2) The maximum acceleration of the isolation object decreases to about 1/3 for El Centro (1940) N-S and to about 1/2 for AKITA (1983) N-S. (3) The isolation effect is not so dependent on the direction of the seismic input. (4) The experimental results are in approximate agreement with the calculated results.

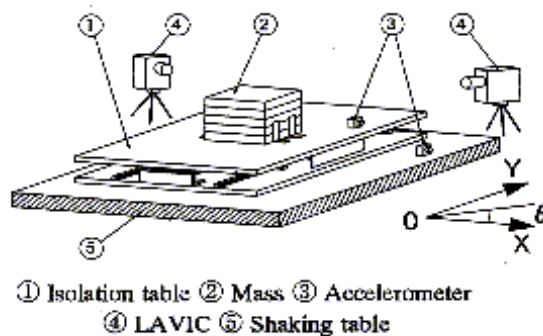


Fig. 11 Experimental apparatus

Table 1 Maxima of the response

Angle $\theta (^{\circ})$	Seismic wave $ \ddot{x}_g _m$ (m/s ²)	El Centro (1940) NS						Akita (1983) NS					
		0.5		1		2		0.5		1		2	
		Exp.	Cal.	Exp.	Cal.	Exp.	Cal.	Exp.	Cal.	Exp.	Cal.	Exp.	Cal.
0°	$ \ddot{x}_1 _m$ (m/s ²)	0.28	0.19	0.39	0.51	0.67	0.99	0.33	0.40	0.88	0.81	1.19	1.62
	$ u_x _m$ (mm)	1.3	1.7	8.7	8.7	19.8	27.0	6.9	7.0	37.0	35.9	76.2	90.9
30°	$ \ddot{x}_1 _m$ (m/s ²)	0.33	0.29	0.39	0.50	0.72	1.12	0.39	0.41	0.83	0.96	1.31	1.10
	$ u_x _m$ (mm)	1.7	1.6	6.4	7.1	20.9	16.3	5.8	6.3	29.8	26.9	70.4	78.2
45°	$ \ddot{x}_1 _m$ (m/s ²)	0.31	0.28	0.39	0.73	0.69	0.82	0.42	0.36	0.83	0.94	1.33	1.10
	$ u_x _m$ (mm)	1.5	1.3	5.7	5.5	20.2	21.9	6.6	4.8	30.4	23.0	73.6	68.9
60°	$ \ddot{x}_1 _m$ (m/s ²)	0.31	0.28	0.39	0.47	0.67	0.75	0.36	0.36	0.78	0.79	1.22	1.03
	$ u_x _m$ (mm)	1.9	1.3	5.7	5.5	15.0	16.3	4.9	3.2	18.8	18.7	65.6	69.7
90°	$ \ddot{x}_1 _m$ (m/s ²)	0.28	0.24	0.36	0.51	0.68	1.01	0.33	0.40	0.81	0.81	1.11	1.79
	$ u_x _m$ (mm)	2.3	1.8	6.1	6.7	17.7	17.8	8.0	5.8	22.5	22.9	84.1	84.7

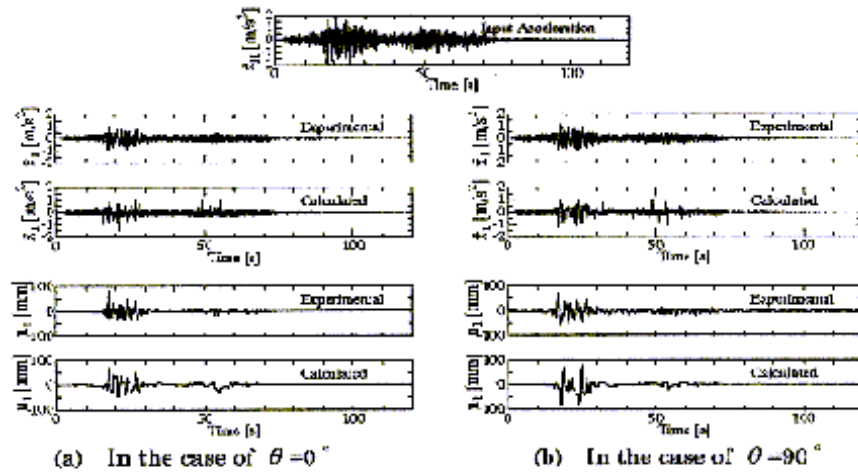
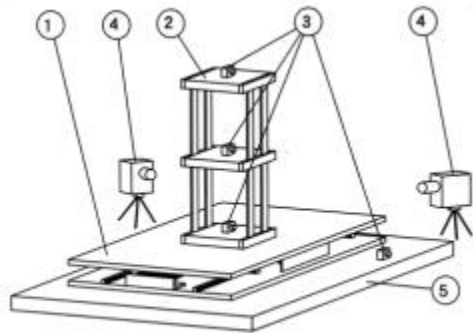


Fig. 12 Response waves (Akita NS)

Case of furnishings model

Figure 13 shows the furnishings model installed on an electro-hydraulic type shaking table. Table 3 shows the experimental and calculated maxima of the acceleration responses \ddot{x}_3 and \ddot{y}_3 , and the displacement responses u_{1x} and u_{1y} for the input seismic waves of El Centro (1940) N-S and AKITA (1983) N-S normalized to be 0.5, 1.0 and 2.0 m/s² at the maximum acceleration. \ddot{x}_3 and \ddot{y}_3 are the responses of the top of the furnishings model, and u_{1x} and u_{1y} are relative responses between the table board and the ground for the seismic input in X and Y direction respectively. Table 3 leads to the following: (1) The effect of the isolation table for El Centro N-S is larger than that of AKITA N-S. (2) The effect of the isolation table becomes larger as the input acceleration increases. (3) The maximum acceleration of the isolation object decreases to about 1/5 to 1/1.5 for AKITA N-S. Figure 14 shows the experimental and calculated response waves for the input of AKITA N-S normalized to be 1.0 m/s² at the maximum acceleration. It can be seen from Fig. 14 that the experimental waves are in approximate agreement with the calculated waves.

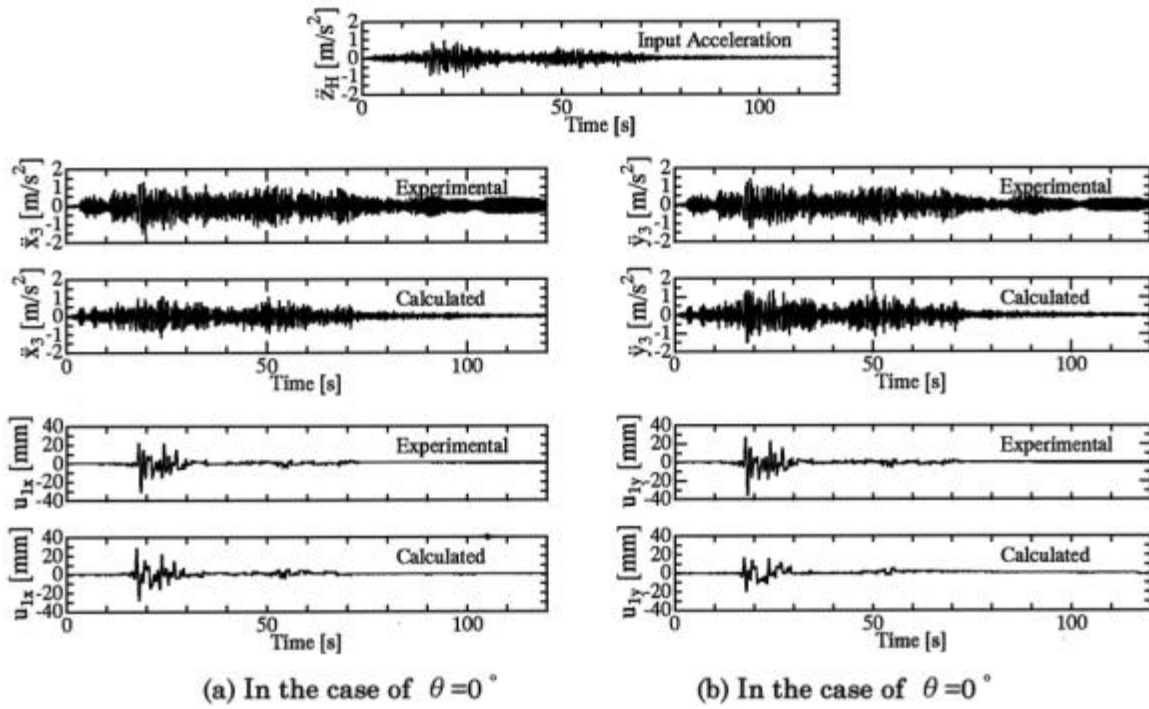
Table 2 Experimental conditions



①Isolation table ②Furniture ③Accelerometer
④LAVIC ⑤Shaking table

X-Y table	Mass	m_0	35 kg
	Damping coefficient	c_x	48 Ns/m
		c_y	80 Ns/m
	Friction coefficient	μ_x	0.014
μ_y		0.014	
Wire rope isolator	Stiffness	k_w	1280 N/m
	Friction	f_w	12.8N
Furniture	Mass	m_1	40 kg
		m_2	30 kg
		m_3	30 kg
	Damping coefficient	c_1	45.4 Ns/m
		c_2	49.4 Ns/m
	Stiffness	k_1	12896 N/m
k_2		12649 N/m	

Fig. 13 Experimental apparatus



(a) In the case of $\theta = 0^\circ$

(b) In the case of $\theta = 0^\circ$

Fig.14 Response waves (Akita NS)

Table 3 Maxima of the response

	Seismic wave $ \bar{z}_n $ (m/s ²)	El Centro (1940) NS				Akita (1983) NS							
		0.5		1.0		0.5		1.0		2.0			
		Exp.	Cal.	Exp.	Cal.	Exp.	Cal.	Exp.	Cal.	Exp.	Cal.		
Without table	$ \bar{x}_3 $ (m/s ²)	2.07	1.98	3.81	3.84	7.87	7.90	3.12	2.78	5.95	5.55	---	11.0
With isolation table	$ \bar{x}_3 $ (m/s ²)	0.91	0.79	1.08	0.95	1.60	1.26	0.98	1.03	1.55	1.72	2.41	2.23
	$ \bar{y}_3 $ (m/s ²)	0.84	0.78	0.98	0.98	1.40	1.19	0.86	1.02	1.40	1.32	2.21	1.69
	$ u_{1x} $ (mm)	2.8	2.4	5.5	6.6	11.2	13.1	6.2	5.4	18.6	20.1	57.0	62.3
	$ u_{1y} $ (mm)	3.3	2.9	7.2	7.3	12.5	13.1	6.8	6.5	35.6	28.3	78.6	70.5

CONCLUSION

Conclusions drawn from the present research are summarized in the following.

- (1) The isolation table has the effect of lowering the acceleration response of the object regardless the direction of seismic excitation in the horizontal plane.
- (2) The maximum acceleration response of the object installed on the isolation table decreases to $1/2$ - $1/3$ to that of the input seismic acceleration in the 0 -800 kg mass range of the object.
- (3) The isolation table has a feature that makes the isolation effect better for larger seismic excitation over the range of the maximum input acceleration from 0.5 to 2.0m/s².
- (4) The isolation table is applicable to the object of which the centre of gravity is in a higher position.
- (5) The wire rope isolator has sufficient fatigue strength for practical applications.
- (6) The experimental results of the acceleration and displacement responses approximately agree with the calculated results.

The authors would like to thank THK Co., Ltd for providing the linear motion ball bearings.

REFERENCES

- Takagami, T., et al. (1986), "Study on an Active Vibration Isolation System", *JSPE* (in Japanese), 52, 5, pp880-886.
- Kashiwazaki, A. and Jinbo, Y. (1989), "The Earthquake and Microtremor Isolation Floor System Utilizing Air Springs and Laminated Rubber Bearings", *JSME* (in Japanese), 55, 512, pp847-852.
- Iwata, Y., et al. (1990), "Active Control of Precision Vibration Isolation System", *JSME* (in Japanese), 57, 534, pp521-526.
- Fujita, S., et al. (1992), "Isolation System for Equipment using Friction Pendulum Bearings (1st Report)", *JSME* (in Japanese), 59, 557, pp11-16.
- Furuya, S., et al. (1992), "An Isolation Table Using Circular Arc Beams and Magnetic Damping", *JSME* (in Japanese), 58, 545, pp56-61.
- Watanabe, K., et al. (1996), "Isolation Table Using Circular Arc Beams and Magnetic Damping", *JSME* (in Japanese), 62, 599, pp2571-2576.